

# Local bending tests & punching failure of a ribbed UHPFRC bridge deck

F. Toutlemonde, J.-C. Renaud & L. Lauvin

*LCPC, Structures Laboratory, Paris, France*

S. Brisard

*SETRA, Bridge Department, Bagneux, France*

J. Resplendino

*CETE de Lyon, Bridge Division, L'Isle d'Abeau, France*

**ABSTRACT:** Local bending tests were carried out on critical locations of a new type of steel-concrete composite bridge deck, as a part of the experimental validation of an innovative ultra-high performance fibre reinforced concrete (UHPFRC) ribbed slab made of segments assembled by post-tensioning. Local failure was identified as one of the possible critical aspects of the design, due to lack of information on the real capacities of UHPFRC materials in bidirectional bending and possible punching shear mechanism. Experimental validation of the design was first derived from the representation of Eurocode wheel models, with a standard 0.4 m x 0.4 m loaded zone. A reduced 0.19 m x 0.26 m had to be used for representing concentrated impacts, and the representation of pavement layers was eliminated, so that the local bearing capacity could be reached. It was finally obtained with a characteristic punching failure mechanism, the ultimate load corresponds to two to three times the nominal wheel load of the Eurocode.

## 1 INTRODUCTION.

### 1.1 *A UHPFRC ribbed slab applied as part of a road bridge deck*

Extending the economic span range of composite bridge decks, classically applied for road bridges from 50 to 100 m-spans, represents an important challenge. For shorter spans, some prototype applications with thinner slabs made of C80 have led to 0.14 m-thick slabs, Causse & Montens (1992), Chevallier & Petitjean (2001). Attempts for even lighter short span bridge solutions using ultra-high performance fiber-reinforced concrete (UHPFRC) are currently under intense study, Tanis (2006), Bouteille et al. (2006).

For longer spans, the concrete slab appears as too heavy, and thinner slabs made of pre-cast high performance concrete (HPC) segments might tend to be developed. This could provide an alternative to steel orthotropic decks, for which fatigue degradations are a major concern. Pursuing this trend of lightness, durability, and savings of natural resources with the use of materials with optimized performance, Bouteille & Resplendino (2005), a preliminary design of a UHPFRC ribbed slab, connected to twin longitudinal steel beams, has been studied within the frame of MIKTI French R & D national project aiming to favor innovative steel-concrete composite applications, Resplendino & Bouteille (2003). The required frame of application consists in a 3-span 90 + 130 + 90 m-long, 9 m-wide road bridge (two 3.5 m-

wide lanes + 1 m-wide side strips) with two 1 m-wide sidewalks. The general design, determination of required pre-stressing tendons and detailing, was carried out applying French Recommendations relative to UHPFRC, AFGC-SETRA (2002) in complement of French Bridge design codes for composite and pre-stressed concrete bridges.

Definition of the slab thickness and of the transverse ribs and pre-tensioning was first determined considering the local and transverse bending. Then longitudinal bending was considered, as well as specific design and connection aspects. Length of successive segments was limited to 2.50 m for possible truck delivery. Regular spacing and similar height of longitudinal ribs was searched, except at the ends for the anchoring of safety barriers. The resulting transverse profile of the deck is represented in Figure 1, and the transverse cross-section of one segment in Figure 2. The current slab thickness is 0.05 m, the total thickness with the ribs is 0.38 m, and the current ribs spacing is 0.6 m from axis to axis in both directions. Current longitudinal ribs are 0.05 m-wide at bottom, 0.1 m-wide at the top. The average resulting weight of the slab is about 3,9 kN/m<sup>2</sup>. Transverse pre-stressing is realized by 2 rectilinear T15S tendons along the vertical axis of the ribs. The upper one is anchored from one end to the other, the lower one is sheathed along the corbels and on supports. The resisting bending moment for a current T-shaped 0.6 m-cross-section is around 115 kN.m, it is limited by the tendons capacity. Longitudinal post-

tensioning ensures a minimum compressive strength equal to 4 MPa for SLS (frequent combination). Low creep of UHPFRC helps keeping the benefit of this post-tensioning very efficiently. An important detailing effort has been carried out for defining anchoring of the safety barrier, connection to the steel main girders, etc. This finally demonstrated the feasibility of realizing a complete bridge design on the basis of AFGC-SETRA UHPFRC Recommendations.

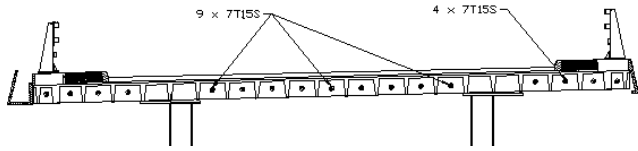


Figure 1. Transverse cross-section including longitudinal post-tensioning (17 strands T15S in sum).

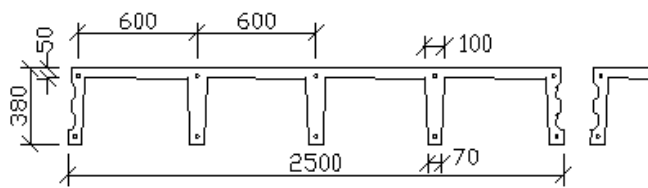


Figure 2. Longitudinal cross-section of precast segments. Longitudinal ribs are 50 mm-wide only at bottom. Lengths in mm.

## 1.2 Experimental validation program

However, before this project can be applied, some critical aspects require validation, since the assumptions of beams theory which have been used at preliminary design stage are questionable regarding local bending and possible partial rotation of the ribs around the loaded honeycombs.

Experimental validation was thus undertaken, Toutlemonde et al. (2005), on a 6.1 m-wide model slab made of two ribbed segments, one made of Ductal®-FM and the other of BSI®, at scale 1 for the length and thickness, connected realistically with a UHPFRC cast in place cold joint and longitudinal post-tension (Fig. 3). Transverse span was reduced to 3.98 m (clear span between longitudinal beams used as simple supports) for bending tests aimed at representing the effects of axle loads, and the cantilever side was used for tests of anchoring of the safety barrier.

Local failure was identified as one of the possible critical aspects of the design, due to lack of information on the real capacities of UHPFRC materials in bidirectional bending and possible punching shear mechanism. Namely, resistance to local bending has a direct implication on the slab thickness (0.05 m) and ribs distance in the project. Experimental validation was first derived from the representation of Eurocode standard wheel models, with a 0.4 x 0.4 m loaded zone. But reduced wheel surfaces should also be considered. Moreover, the favourable effect of pavement layers should be quantified.



Figure 3. Model ribbed slab for validation tests. a) Casting – b) Cold joint – c) Honeycombs ; in the center, the connected side ribs of the segments – d) Longitudinal post-tensioning – e) Overview of the model under general ‘axle’ bending test.

## 2 LOCAL BENDING TESTS

### 2.1 Loading setup and objectives

The local bending tests should help quantifying the effective bearing capacity with respect to possibly concentrated loads over the bridge deck. The loads should thus be concentrated at the centre of one particular honeycomb, where the deck is at the thinnest. This location corresponds to the conventional design situation. Assuming  $45^\circ$  diffusion through 9 cm-thick bituminous concrete pavement layers and the deck slab, this design case with a 150-kN service live load according to Eurocode 1 appears as critical with respect to the tensile strength of UHPFRC at the centre of the honeycomb lower sides.

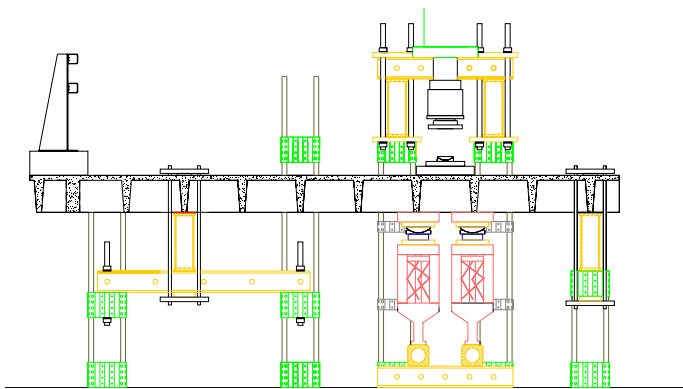


Figure 4. Transverse cross-section of the model in the local bending tests configuration.

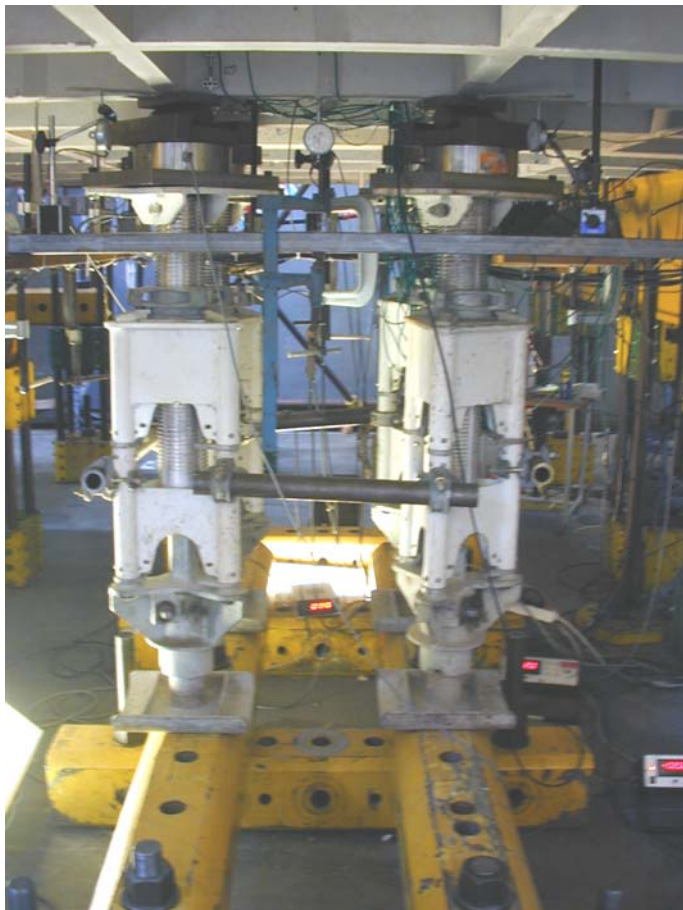


Figure 5. Supporting stays at corners of the loaded honeycomb.

For the experimental validation, since this phase should be at least locally destructive, it was carried out after the fatigue resistance verification described in Toutlemonde et al. (2007). The 3.98 m-span transverse support system was kept, however intermediate supports at the four corners of the loaded honeycomb were provided, so that the load applied by the actuator could be significantly taken by the reactions of the 4 stays (Fig. 4-5). Free rotation was permitted on each support towards the centre of the honeycomb using an intermediate roll, and the reaction on each stay was measured using a load cell (Fig. 6). The test was load-controlled during a first linear phase with a loading rate of 1 kN/s, then the actuator displacement was used as the load-control signal with a reference  $10 \mu\text{m/s}$  rate. The testing capacity was limited by the stays (200 kN maximum on each) or the actuator (1000 kN).



Figure 6. Support detail and reaction load measurement.

### 2.2 Tested zones

The tested honeycombs were chosen so that the results could integrate the influence of the UHPFRC material (Ductal®-FM or BSI®), the influence of the twin transverse key rib with cold joint, which can be one side of the loaded honeycomb, and the possible influence of previous fatigue cyclic program, even though it has been shown as non-damaging for the structure, Toutlemonde et al. 2007.

Four honeycombs were thus chosen for the tests (Fig. 7). They are aligned between longitudinal ribs NL8 and NL9 so that the actuator can be easily moved over the zones to be tested, due to its fixation on longitudinal steel rectangular girders 6 m-long over the model (Fig. 8). This choice was also necessary for adapting the supporting system of stays under the slab (Fig. 5). Ends of the slab were avoided, thus the tested zones were limited in the longitudinal direction by transverse ribs referred as N2 and N3, N3 and N4, N5 and N6, and N6 and N7. It was thus expected to get some statistical relevance of the ultimate loading capacity experimentally identified.

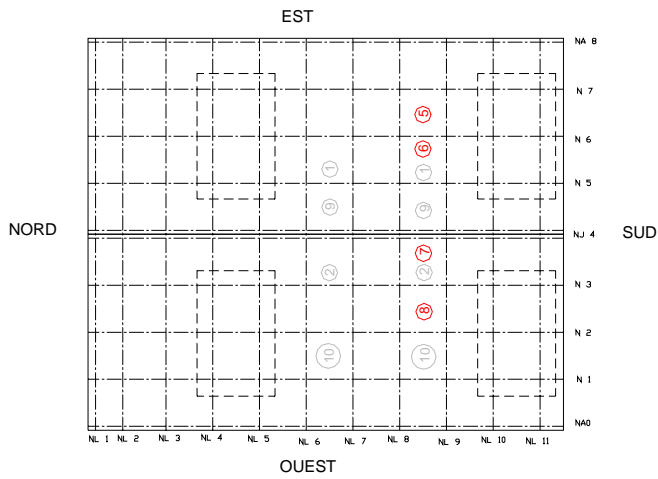


Figure 7. Location of local bending tests (dark circles).



Figure 9. Load distribution: Configuration 1.



Figure 8. Fixation of the actuator and superstructures.

### 2.3 Load diffusion configurations

In the reference case corresponding to the bridge project, referred to as ‘configuration 1’, application of the ‘wheel’ load included a 0.09 m-thick polymer material (PA6 commercially available as  $\text{\textcircled{E}}\text{rtalon}$ ) 0.6 m-square plate, representative of the diffusion induced by the bituminous concrete paving layers. Young’s modulus of this material is about 2.5 to 3 GPa, close to an average value of bituminous concrete (which highly depends on temperature). For correct load distribution between the rough UHPFRC slab and the  $\text{\textcircled{E}}\text{rtalon}$  plate confined sand is provided. Over this plate, the load was distributed over a surface deriving from Eurocode 1 wheel model. The reference surface is 0.4 x 0.4 m corresponding to fatigue load models 1 and 3. It is represented in the tests below a point ball hinge under the jack end by a 0.4 x 0.4 x 0.04 m steel plate (Fig. 9).

However, reduced surfaces are also considered in Eurocode 1 fatigue load models #2 and 4, with wheel types A and C (0.22 x 0.32 m or 0.27 x 0.32 m). Similarly to the fatigue testing program, Toutlemonde et al. (2007), a reduced steel plate of dimensions 0.19 x 0.26 x 0.04 m with corners cut at 2 cm was used instead of the 0.4 m-square one in ‘configuration 2’ (Fig. 10). The longer side is along the longitudinal direction.

Due to the very low porosity of UHPFRC materials, which might permit to consider bridge decks without watertight and paving overlays, and for a safe evaluation of the slab capacity, tests were also carried out without the 0.09 m-thick polymer layer, possibly representing transient phases where the bridge deck has not got any pavement layer. ‘Configurations 3 and 4’ correspond to such situations with the standard or reduced wheel surfaces, respectively (Fig. 11-12). Under the steel plate, confined sand under a 3 mm-thin cardboard is still provided.



Figure 10. Load distribution: Configuration 2.



Figure 11. Load distribution: Configuration 3.



Figure 12. Load distribution: Configuration 4.

## 2.4 Synthesis of tests carried out

A summary of the test configurations and locations is given in Table 1. The first two zones (N5N6 and N3N4) correspond to honeycombs previously submitted to fatigue loading as described in Toutlemonde et al. (2007). Especially, 100,000 cycles between 5 and 155 kN had been applied on each of these zones under ‘configuration 2’. The local bending tests were carried out from June 2006 to September 2006. The ribbed slab was about 2 years old. Eighty measurement channels were used in order to characterize the global and local bending of the ribbed slab, local strains, deflection at the centre of the honeycombs, vertical displacement at the corners and at mid-span of the loaded honeycomb side ribs. In the following focus is given on the major results in terms of load, deflection and failure modes.

The materials of which the model was made had already been used in real structures, St-Pierre-la-Cour bridge or the roof of Millau bridge tollgate, Bouteille & Resplendino (2005). One segment is made of Ductal®-FM, having a water to cement ratio equal to 0.21 and a volumetric fiber content equal to 2.15 %. Thermal treatment was applied at an age of 48 h, consisting in 48 hours exposure at 90°C and 95% RH. Average compressive strength measured on cylinders, 70 mm in diameter, is 190 MPa. Aver-

age specific gravity determined on the same specimens is 2.53 kg/m<sup>3</sup>, Young’s modulus 55 GPa and Poisson’s ratio 0.17. Ductal®-FM characteristics in tension were identified on six 0.05 x 0.20 x 0.6 m plates tested under 4-point bending with a 0.42 m clear span according to ‘thin plates’ procedure of UHPFRC Recommendations, AFGC-SETRA (2002). Average limit of linearity ‘ftj’ identified on these specimens corresponds to 9.8 MPa (mean value). The conventional ‘ftu’ value which helps accounting for the maximum bending moment of these plates is 9.5 MPa (mean value).

The other segment is made of BSI®. Average compressive strength measured after 2 years on cylinders, 110 mm in diameter, is 219 MPa. Young’s modulus is 68. Using ‘thin plates’ bending tests for determining the design constitutive tensile behavior leads to a limit of linearity ‘ftj’ equal to 9.3 MPa (mean value). The conventional ‘ftu’ value which helps accounting for the maximum bending moment of the plates is 8.3 MPa (mean value).

Table 1. Test configurations and locations (N4 is the joint).

Date	Zone	Material	Config.	Result
Jun 14	N5N6	Ductal®-FM	1	limit of stays capacity
Jun 15	N5N6	Ductal®-FM	2	limit of stays capacity
Jun 26	N5N6	Ductal®-FM	3	limit of stays capacity
Jun 26	N5N6	Ductal®-FM	4	punching shear failure
Jul 12	N3N4	BSI®	4	punching shear failure
Aug 22	N2N3	BSI®	3	limit of stays capacity
Jul 12	N2N3	BSI®	4	punching shear failure
Sept 15	N6N7	Ductal®-FM	4	punching shear failure

## 3 GLOBAL RESULTS

### 3.1 Progress of the experimental program

Before each test, stays were adjusted so that about 90 % of the slab dead weight (4 x 30 kN) is taken by the stays, and contact of the actuator was ensured with 10 kN-pre-load. Then, due to stays and model compliances, about 60 % of the actuator load is taken by reaction of the stays, while the remaining load leads mostly to general transverse bending of the slab. In these tests no irreversible degradation was observed due to this residual transverse bending, on the contrary it was searched, in using the different configurations, to focus on local damage. Therefore only the total reaction load (sum of the loads taken by the stays) is considered in the following as significant for the local honeycomb behavior.

Local failure which was searched could be obtained neither with configurations 1, 2 nor 3, even though the total reaction reached about 700 kN, both on Ductal®-FM and BSI® zones. For zone N5N6 significant non-linear extension was observed with configuration 1 beyond 300 kN, but whatever configurations 1 to 3, bending cracks only 0.2 mm-wide were opened with a 700 kN total local load. For

zone N2N3 the bending damage signs under 700 kN were not so diffuse: diagonal ‘yield lines’ had been initiated beyond ca. 400 kN from the center to corners of the loaded honeycomb. Residual deflection however did not exceed 0.4 mm. Finally only with configuration 4 the maximum local bearing capacity could be reached over all tested zones. Next sections consider the observed failure mode and loads.

### 3.2 Tests having reached failure : failure mode

Punching shear failure was observed in all cases as shown in Figures 13 to 16. On top of the slab, the critical crack reaches roughly the limits of the loading plate (Fig. 14), even after previous other loading configurations (Fig. 13a, Fig. 17). From lower side, failure is located at the inner edge between the ribs and the top slab. Cracks due to bending are visible especially for zone N5N6 (Fig.13b), where they are very fine and diffuse due to the progressive configuration variation, and zone N2N3 (Fig. 15b) where they are concentrated in a yield line pattern. Only for zone N6N7 rotation was observed on one smaller side (Fig 16a). Otherwise, the failure pattern was fully symmetrical. For zone N3N4 it was even possible to isolate the failed punched element (Fig. 18).



Figure 14. Punching shear failure. Zone N3N4. Top side.



Figure 15. Punching shear failure. Zone N2N3. a) Top side. b) Bottom side.

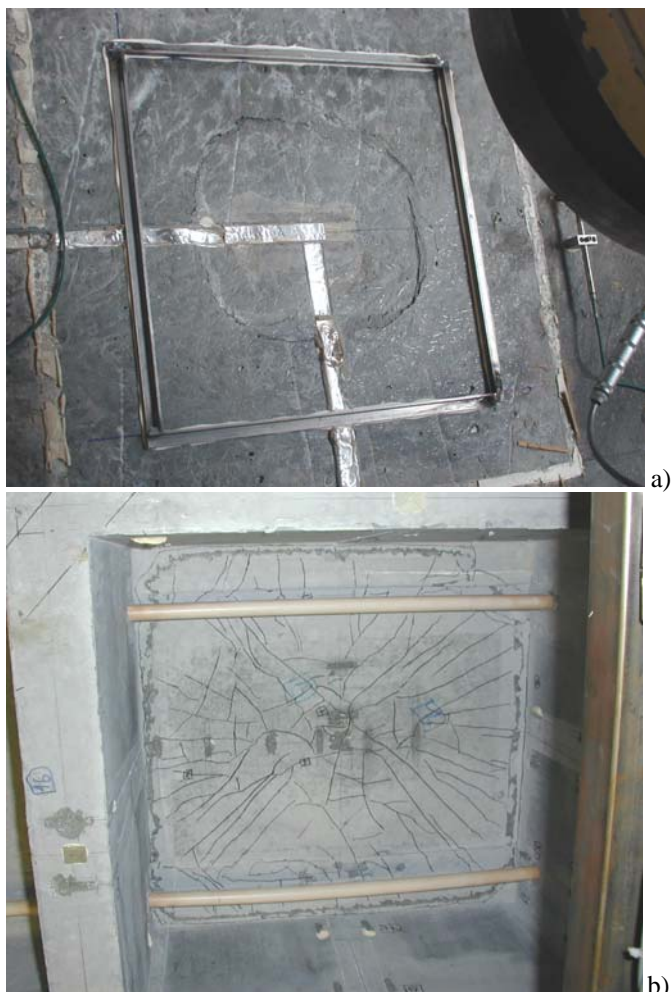


Figure 13. Punching shear failure. Zone N5N6. a) Top side. b) Bottom side.

Referring to classical schemes of shear mechanisms, the shape of the failed element corresponds to very inclined struts. This may be induced by the rigid frame constituted by the ribs. When the top slab is loaded, membrane tensile stresses due to this frame may be superimposed to bending and shear stresses. Moreover, the fiber distribution and orientation are probably disturbed at the inner edges between ribs and the top slab, which may tend to focus the basis of shear inclined cracks at this location.



Figure 16. Punching shear failure. Zone N6N7. a) Top side. b) Bottom side.

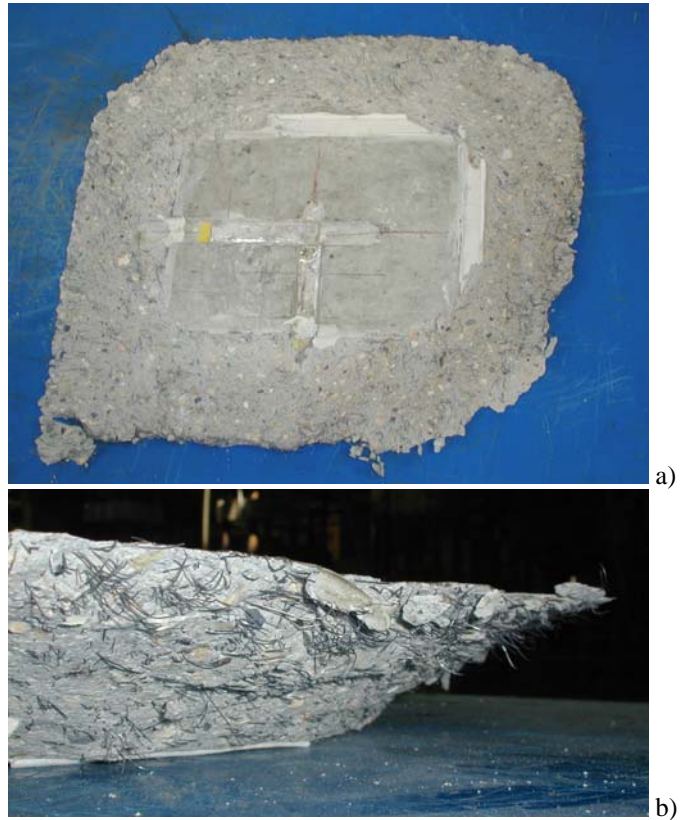


Figure 18. Punching shear failure. Zone N3N4. a) The punched slab piece from top side. b) Fibers pulled out at the edge.



Figure 17. left) Zone N2N3 after failure. Failure on top is concentrated around the reduced loading plate even with sand cushion over the 0.4 m-square surface (configuration 3). Right) Zone N3N4 after failure (configuration 4).

### 3.3 Failure loads

Failure loads (in terms of total reaction on the stays) range from 352 to 417 kN (Fig. 19). Previous loading configurations and fatigue cycles pre-loading did not induce any bearing capacity reduction, as induced from comparisons of zone N5N6 (Fail\_test1) vs. zone N6N7 (Fail\_test4), and zone N3N4 (Fail\_test2) vs. zone N2N3 (Fail\_test3), respectively.

The failure loads are on average 12 % higher for the zones of the Ductal®-FM segment (417 and 391 kN vs. 365 and 352 kN), which may be consistent with the slightly higher tensile characteristics of this UHPFRC material. When referring this punching load to the vertical cross-section along the loading surface (0.05 m thickness x 0.85 m perimeter of the plate), a shear stress value of 8.3 to 9.8 MPa is obtained, which is close to the direct tensile strength of the UHPFRC materials. This indication may be useful for further design rules, due to the lack of other experimental results under such failure modes.

From the load-central deflection curves (Fig. 19) the non-linear behavior of loaded zones of the BSI® segment turns out visible for loads exceeding 180 kN, and the stiffness reduction is more pronounced. This is probably consistent with a more ductile tensile post-peak behavior of Ductal®-FM as identified on thin plates under bending, and could be related to its higher number of thinner fibers. However in all cases the punching shear failure takes place very suddenly and leads to a dramatic load decrease and deflection increase.

From the designer's point of view, the safety factor on the maximum concentrated load (150 kN for LM1 in Eurocode 1) ranges from 2.35 to 2.78. If a maximum local pressure of 1125 kN/m<sup>2</sup> is considered (parking loads), the safety factor reaches 6. Concerning the maximum shear force around the concentrated load, maximum design value of Eurocode 1 (LM2) reaches 105 kN/m, the safety factor is thus about 4.6.

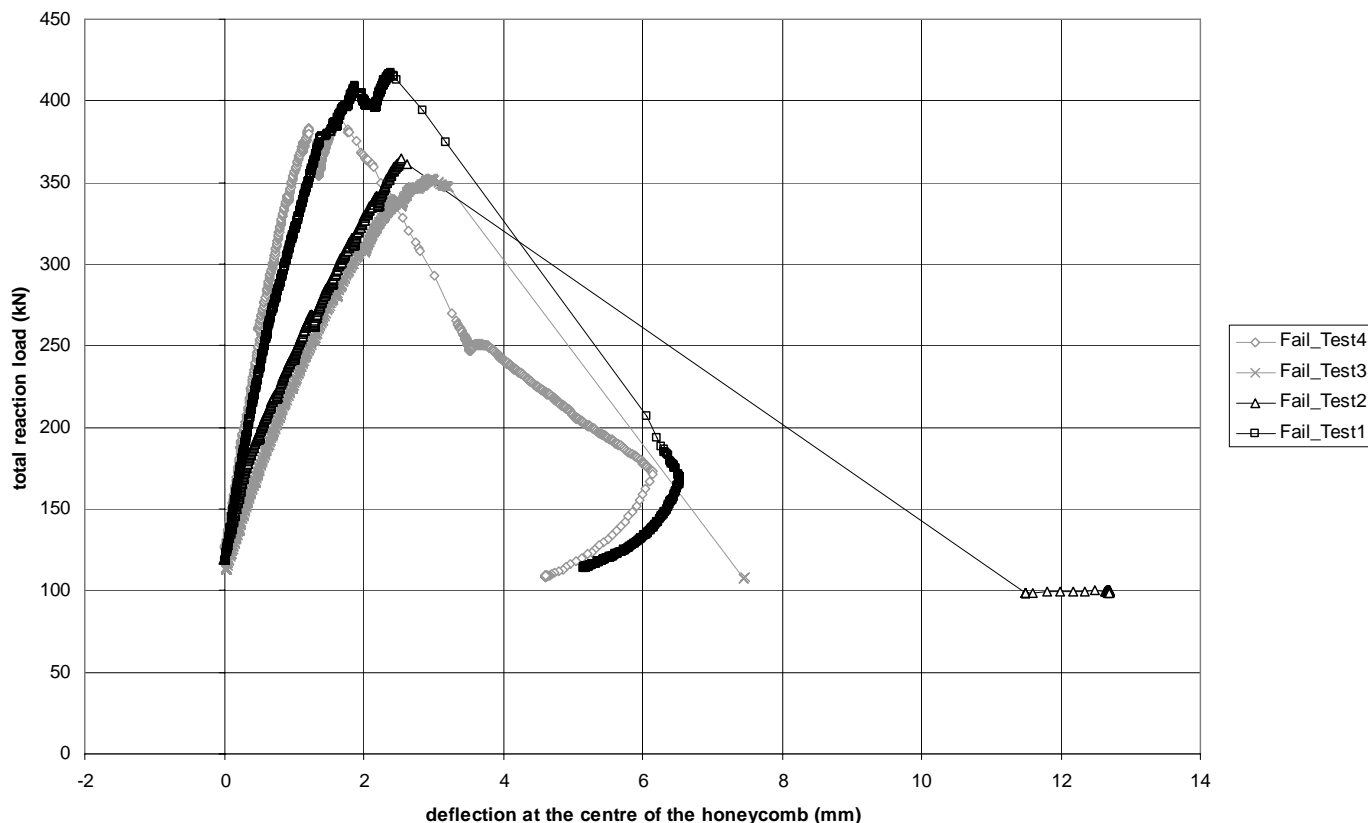


Figure 19. Global load / deflection behavior during tests having reached punching shear failure

#### 4 CONCLUSION

Experimental validation of an innovative design of UHPFRC ribbed slab was carried out, regarding local capacity over 0.05 m-thick, 0.6 m-wide honeycombs. When diffusion was ensured efficiently enough towards the ribs, no local failure was obtained even with loads up to 700 kN. When the surface of load application was reduced enough, punching shear failure was obtained for loads reaching about 2.5 times the Eurocode design load, with a mean shear stress along the load surface close to the tensile strength of the UHPFRC material.

#### 5 ACKNOWLEDGEMENT

This experimental program has been carried out within the R&D “National Project” MIKTI, funded by the Ministry for Public Works (DRAST / RGCU) and managed by IREX. It has been supervised by a committee chaired by J. Resplendino (CETE de Lyon), also chairman of the *fib* TG 8.6 mirror group. Eiffage Construction (A. Simon) and Lafarge (M. Behloul) are gratefully acknowledged for their contribution in the specimen preparation. The authors are pleased to thank M. Estivin, J. Billo and F.-X. Barin from LCPC Structures Laboratory for their help in the experimental realizations.

#### REFERENCES

- Eurocode 1 – Partie 2: Actions sur les ponts, dues au trafic, NF EN 1991-2:2004
- AFGC-SETRA 2002. *Ultra High Performance Fibre-Reinforced Concretes. Interim Recommendations*. Bagnaux: SETRA.
- Bouteille S. & Resplendino J. 2005. Derniers développements dans l'utilisation des bétons fibrés ultra-performants en France. In *Performance, Durabilité, esthétique, Proc. GC'2005, Paris, 5-6 October 2005*. Paris: AFGC.
- Bouteille S., Le François M., Resplendino J. 2006. Etude de solutions composites BFUP – matériau composite – acier. *European project NR2C. WP3 report*. CETE de Lyon.
- Causse G. & Montens S. 1992. The Roize Bridge, *High Performance Concrete. From material to structure*. E & FN SPON, 525-536.
- Chevallier F. & Petitjean J. 2001. A85. Le PS 13. Les ouvrages mixtes à dalle préfabriquée en BHP. *Travaux*. **771**.
- Resplendino J. & Bouteille S. 2003. PN MIKTI. Etude d'un pont mixte à dalle BFUP nervurée. *CETE de Lyon. technical report*, 46 p.
- Tanis J.-M. 2006. Quelles structures pour demain ? In *Proc. Coll. Interoute, Session A2 « NR2C », Rennes (France), 24-26 October 2006*.
- Toutlemonde F. et al. 2005. Innovative design of ultra-high performance fiber-reinforced concrete ribbed slab : experimental validation and preliminary detailed analyses. In Henry Russel (ed.), *Proc. 7<sup>th</sup> Int. Symp. On Utilization of High Strength / High Performance Concrete, Washington D.C. (USA), 20-22 June 2005*. ACI-SP 228, 1187-1206.
- Toutlemonde F. et al. 2007. Fatigue performance of UHPFRC ribbed slab applied as a road bridge deck verified according to Eurocodes, In *Proc. 5<sup>th</sup> Int. Conf. On Concrete under Severe Conditions CONSEC'07, Tours (France), 4-6 June 2007*.